4209

Theoretical Basis of Primitive Part Modeling

Tin-Tai Chow, Ph.D., C.Eng.
Member ASHRAE

Joseph A. Clarke, Ph.D., C.Eng.

ABSTRACT

At the present time, the simulation of buildings and their environmental control systems is enjoying growing acceptance by practitioners worldwide. At the same time, these same programs possess internal structures and modeling approaches that will restrict future extensibility in response to growing user expectations. This situation is particularly problematic in relation to the modeling of HVAC systems, where inflexible component algorithms will restrict applications to standard and conventional system configurations. One reaction to this issue is to move toward a process-oriented representation of the HVAC component models. In this approach, a library of "primitive parts" (PP) is established where each PP describes (mathematically) an elementary heat, mass, or mixed transfer process. HVAC system component models may then be synthesized at simulation time from appropriate PP combinations. This paper explains the PP approach and illustrates its application to practical problems.

INTRODUCTION

The consequence of mechanically supplying or removing heat from a space depends on several factors, such as the thermal response of the fabric and contents, occupant behavior, air movement regimes, HVAC system capabilities, and control system behavior. Taken together, these factors give rise to a system that is nonlinear, time varying, and systemic (in that there are many causal interactions). Such a system requires special mathematical modeling procedures and numerical integration methods (e.g., Clarke 1985). Figure 1 illustrates this complexity as typically found within HVAC systems.

Where applicable, simulation provides a most powerful tool for the appraisal of HVAC systems in the dynamic (i.e., realistic) domain. The technique can be applied to assist in equipment sizing and selection, to support design optimization, and to compare alternative approaches. Unfortunately, simulation programs are not unconditionally applicable because of inherent assumptions and inflexible component models. They are, therefore, unable to deal with the range of problems likely to be encountered in practice (Sowell 1991).

At the present time, simulation is evolving toward an approach that offers full building and HVAC system integration, based on a fundamental mathematical approach. When a model is built up from the mathematical descriptions of basic energy and mass transfer phenomena, the need for experiments is not apparent. Models can be constructed to the point where all but a few key relations or parameters are known, then valuable experiments can be carried out to determine these unknown quantities (Mitchell 1997). A complementary goal is to achieve an approach to HVAC component modeling that offers program interoperability and helps to converge the disparate theories. This goal is apparent within several contemporary developments, such as the neutral model format (NMF) project (Bring et al. 1992; Sahlin et al. 1995), the input-output independent models of the SPARK system (Buhl et al. 1993; Sowell and Moshier 1995), and the primitive parts (PP) approach within the ESP-r system (Clarke 1985; Chow 1993, 1995).

PP and NMF are basically different in that PPs are elemental mathematical models whereas NMF is a model description method. PP modeling is an innovation that allows modelers, in the short term, to construct component models from a finite set of elemental process models and, in the longer term, for this to be achieved automatically at run-time as the need arises. The principal advantage of the PP approach is its flexibility in generating component models for the multiplicity of possible plant systems and modeling abstractions. Alternative input-output relationships are represented by different

Tin-Tai Chow is a principal lecturer in the Division of Building Science and Technology, City University of Hong Kong, China. **Joseph A. Clarke** is a professor and the director of the Energy Systems Research Unit, University of Strathclyde, Scotland.

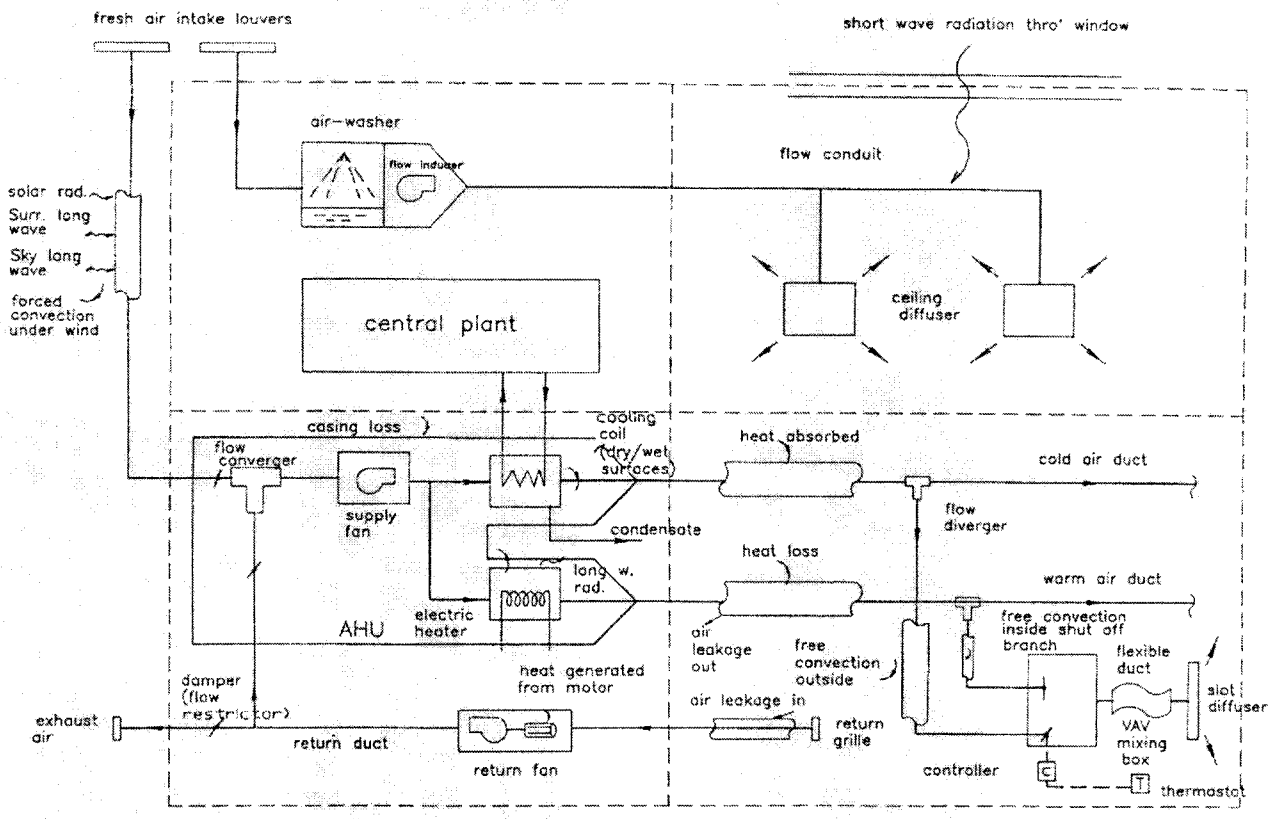

Figure 1 *Energy and mass flow paths in air-conditioning systems.*

PP groupings arranged automatically at the point of component model selection (Chow et al. 1997).

The developmental work to date has been based on the finite volume conservation method, by which a dynamic model may be constructed that conserves system integrity by numerically processing all elements of the problem as a state-connected system.The ultimate aim is to support the automatic formulation of component mathematical models on the basis of explicit descriptions of components as distinct from an approach in which preconstructed models are links to define a system. The former approach is deemed to be more flexible and so able to accommodate a wide range of component types.

FINITE VOLUME CONSERVATION METHOD

In the context of the ESP-r system, the finite volume conservation method was first applied to dynamic building/plant modeling in the late 1970s, continuing to the present day (Clarke 1977; McLean 1982; Tang 1985; Clarke 1986; Clarke and Mac Randal 1993; Aasem 1993). In the approach, plant components are physically decomposed into a finite number of subparts, or control volumes (CV). A CV can be homogeneous, and, therefore, possess uniform hygrothermal properties, or heterogeneous, and, therefore, possess a set of hygrothermal properties. In both cases, the region represented by the CV has a single set of state variables (enthalpy, pressure, voltage, mass, etc.).

For each CV in turn, and in terms of all other CVs in potential thermal, electrical, or flow contact, conservation equations are developed in relation to the transport properties of interest (heat energy and fluid exchange, for example). The arbitrariness of CV discretization allows the technique to be applied to objects with irregular shapes and subject to multi-dimensional, mixed-mode heat and mass transfer.

Consider an arbitrary CV, i, representing a single-phase fluid as shown in Figure 2. For this case, the energy and mass balance equations are given by

$$m_{i-1}Cp_{i-1}\theta_{i-1} - m_iCp_i\theta_i + Q = \frac{\partial}{\partial t}(M_iCp_i\theta_i) \qquad (1)$$

and

$$m_{i-1} - m_i = \frac{\partial}{\partial t}(M_i) \qquad (2)$$

where m is the fluid flow rate (kg/s), Cp is the fluid specific heat (J/Kg.K), θ is temperature (°C), M is the mass (kg), and Q is the rate of heat addition (W); i-1 relates to the upstream CV connected to i.

The time-variant θ and Cp in Equation 1 are the spatially averaged values within a CV. For solid CVs, Equation 2 is

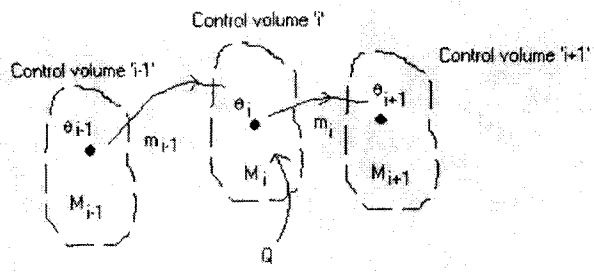

Figure 2 Control volume energy and fluid flow.

omitted, while a multiphase flow problem (e.g., the dry air and vapor phases within an air-conditioning system) will require a mass balance equation for each phase. Within ESP-r, the CV conservation equations are made time discrete by application of finite differencing (Clarke 1985). For a small time interval δt, Equation 1 can be expressed in the explicit, implicit, or Crank-Nicolson formulations, respectively, as follows:

$$m^*_{i-1} Cp^*_{i-1} \theta^*_{i-1} - m^*_i Cp^*_i \theta^*_i + Q^* = M^*_i Cp^*_i \left(\frac{\theta_i - \theta^*_i}{\delta t}\right) \quad (3a)$$

$$m_{i-1} Cp_{i-1} \theta_{i-1} - m_i Cp_i \theta_i + Q = M_i Cp \left(\frac{\theta_i - \theta^*_i}{\partial t}\right) \quad (3b)$$

$$\left(\frac{m_{i-1} Cp_{i-1} \theta_{i-1} + m^*_{i-1} Cp^*_{i-1} \theta^*_{i-1}}{2}\right) - \left(\frac{m_i Cp_i \theta_i + m^*_i Cp^*_i \theta^*_i}{2}\right) + \left(\frac{Q + Q^*}{2}\right) = \left(\frac{M_i Cp_i + M^*_i Cp^*_i}{2}\right)\left(\frac{\theta_i - \theta^*_i}{\delta t}\right) \quad (3c)$$

where * signifies quantity evaluation at the present (known) time-row of some arbitrary time-step (all other quantities relate to the future, unknown time-row). The above three equations can also be represented in a generalized form, as shown below, by a weighting factor α, which defines the degree of "implicitness" of the equation: 0, 1, and 0.5 corresponding to the explicit, implicit, and Crank-Nicolson weighted average cases, respectively, taking the CV thermal mass as time invariant.

$$\left[-\alpha m_i - \frac{M_i}{\delta t}\right] Cp_i \theta_i + \alpha m_{i-1} Cp_{i-1} \theta_{i-1} = \left[(1-\alpha) m^*_i - \frac{M_i}{\delta t}\right] Cp^*_i \theta^*_i + (1-\alpha) m^*_{i-1} Cp^*_{i-1} + \alpha Q + (1-\alpha) Q^* \quad (3d)$$

PLANT MATRIX EQUATION

Any HVAC system can, therefore, be represented as a network of nodes (the CVs) connected by arcs (the conservation equations linking CVs). In an air-conditioning system, for example, each CV will therefore be described by three conservation equations corresponding to energy and two-phase mass balance. The collection of such equations for the nodes (CVs) composing a single component gives rise to a generic mathematical model for that component type. It is the job of the run-time simulator to synthesis the overall plant matrix equation from the individual component models composing the overall network. This requires knowledge of the factors influencing the CVs and a means to evaluate the equation coefficients at each time-step.

Control equations are then added to the matrix equation to prescribe or limit parameter values before the entire equation set is passed to the solver for time-step integration. For an integrated building and plant problem, the solution procedure utilizes several solvers operating in tandem, each one customized to a particular subsystem, e.g., piecewise, direct inversion of linearized equations describing energy and mass balance and iterative solvers for fluid flow (Clarke 1985). Where possible, nonlinear equations are linearized by absorbing the nonlinear elements into the variable coefficients and employing iteration.

The essential consequence of linearization on the plant side is that the principle of superposition can then be applied. It is the application of this principle that gives rise to the theory of primitive parts.

THEORY OF PRIMITIVE PARTS

Consider Figure 3, which shows a surface, S, in conductive contact with a region X, in convective contact with a region Y, and in radiative contact with a region Z. The energy balance equation for S is given by

$$C_{sx}(\theta_x - \theta_s) + C_{sy}(\theta_y - \theta_s) + C_{sz}(\theta_z - \theta_s) = M_s C_s \frac{d\theta_s}{dt} \quad (4)$$

where $C_{sx} = k_{sx} A_{sx} / l_{sx}$, $C_{sy} = h_{sy} A_{sy}$, and $C_{sz} = h_{sz} A_{sz}$. Applying a finite difference approximation to the time derivative gives

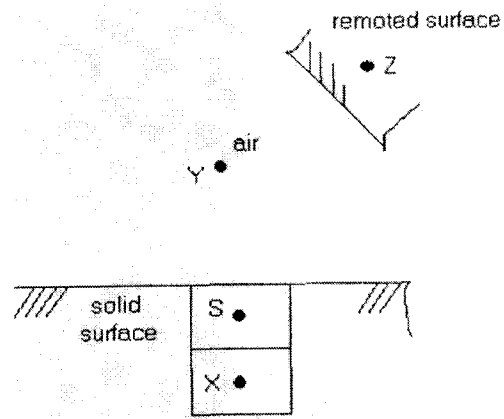

Figure 3 Discretization scheme for surface node "S."

$$\left[-\alpha(C_{sx}+C_{sy}+C_{sz})-\frac{M_s C_s}{\delta t}\right]\theta_s+\alpha C_{sx}\theta_x+\alpha C_{sy}\theta_y+\alpha C_{sz}\theta_z=\left[(1-\alpha)(C^*_{sx}+C^*_{sy}+C^*_{sz})-\frac{M^*_s C^*_s}{\delta t}\right]\theta^*_s-(1-\alpha)C^*_{sx}\theta^*_x-(1-\alpha)C^*_{sy}\theta^*_y-(1-\alpha)C^*_{sz}\theta^*_z \quad (5)$$

where * denotes the present time row ($M_s = M_s^*$ for most practical applications).

Equation 5 can be rewritten in its matrix equation form:

$$[C(1)C(2)C(3)C(4)]\cdot\begin{bmatrix}\theta_s\\ \theta_x\\ \theta_y\\ \theta_z\end{bmatrix}=[C(5)] \quad (6)$$

In ESP-r's conventional, component-centered approach, pre-constructed routines of various plant components exist to generate the numerical values of a component's equation coefficients at each time-step, i.e., $C(1)$ through $C(5)$ in Equation 6, for transmission to a central matrix equation construction and solution controller (i.e., the simulation engine). However, by the principle of superposition, it is possible to synthesis component models from a common set of primitive parts so that the need for pre-formed component models is eliminated. This significantly increases program applicability and reduces complexity.

Table 1 lists the primitive parts (PPs) now available for use by ESP-r and gives an example application in each case. These PPs are grouped under ten categories and numbered accordingly. For the current component, three PPs are involved:

PP	Description	Nodes Involved
1.1	Thermal conduction: solid to solid	S, X
2.1	Surface convection: with moist air	S, Y
3.1	Surface radiation: with local surface	S, Z

While the matrix equations underlying the above PPs, and another six as employed in this paper, are given in the Appendix, a full description of the entire family of 27 is given elsewhere (Chow 1995b). Within a PP matrix equation, each $A(i,j)$ represents a future time-row coefficient of a nonhomogeneous matrix of the nodal temperature/mass flow rates; $B(i,j)$ represents a present time-row coefficient of the corresponding matrix, absorbed with the known boundary excitations relating to both the present and future time-rows.

The rule of superposition (Ogata 1992) may then be applied by which each matrix equation coefficient is determined as the sum of constituent PP equation coefficients. Hence, in the current problem:

$$C(1) = A(11,1)+A(21,1)+A(31,1) = -\alpha(C_{sx}+C_{sy}+C_{sz})-M_sC_s/\delta t$$

$$C(2) = A(11,2) = \alpha C_{sx}$$

$$C(3) = A(21,2) = \alpha C_{sy}$$

$$C(4) = A(31,2) = \alpha C_{sz}$$

$$C(5) = B(11,1)+B(21,1)+B(31,1) = [(1-\alpha)(C_{sx}^*+C_{sy}^*+C_{sz}^*)-M_s^*.C_s^*/\delta t]\,\theta_s^*-(1-\alpha)C_{sx}^*\theta_x^*-(1-\alpha)C_{sy}^*\theta_y^*-(1-\alpha)C_{sz}^*\theta_z^*.$$

These relationship are identical to those that would result from first principle considerations applied to Equation 5. A key parameter in PP modeling is Ni, defined as the "primitive part connection index" (hereinafter, the "PP index") of a particular node. This index indicates the number of PPs used in describing the energy/mass flow paths involving the thermal mass of the particular node. In this case, the number of participating PPs for the node S is 3; hence, Ni_s is equal to 3. The specific role of Ni_s is to maintain the thermal capacitance of S equal to $M_s \cdot C_s$ and, therefore, make the capacitance term independent of the number of PPs participating in the addition process.

The PP approach is further illustrated in the following section, where two practical examples are considered.

AIR DUCT MODEL

A section of an insulated air duct is arbitrarily discretized into four finite volumes as shown in Figure 4. Two of these, denoted by nodes S1 and S2, represent the thermal insulation and the sheet metal, respectively; node AM represents the air inside the duct; and nodes A0 and A1 represent the entering and leaving air states and are used to connect to the upstream and downstream components, respectively. This arrangement facilitates the modeling of the transport delay phenomenon where necessary. In the following derivation, no transport delay is first assumed for simplicity.

Assuming that the ambient energy exchange takes place with a known boundary condition, θ_e, the energy conservation equations for the four nodes are as follows.

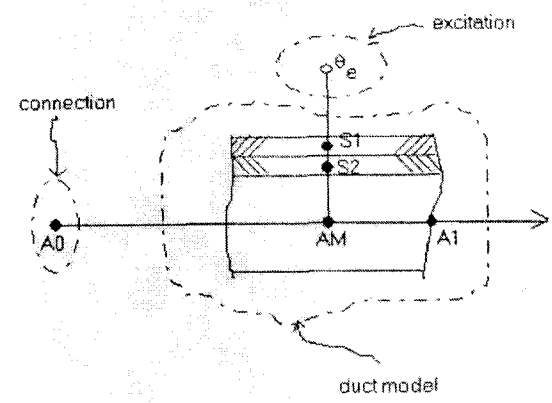

Figure 4 Four-node insulated air duct.

TABLE 1
List of Primitive Parts

Categories		Application Examples
1	**Thermal Conduction**	
1.1	Solid to Solid	Pipe wall with thermal insulation
1.2	With Ambient Solid	Duct hanger attached to building structure
2	**Surface Convection**	
2.1	With Moist Air	Cooled-ceiling and room air
2.2	With 2-Phase Fluid	Refrigerant and condenser shell surface
2.3	With 1-Phase Fluid	Hot-water boiler interior surface
2.4	With Ambient	Outdoor air-duct exterior surface
3	**Surface Radiation**	
3.1	With Local Surface	Heater element and its casing inner surface
3.2	With Ambient Surface	Radiator and room surface
4	**Flow Upon Surface**	
4.1	For Moist Air; 3 Nodes	Air flow in duct
4.2	For 2-Phase Fluid; 3 Nodes	Wet steam flow in pipe
4.3	For 1-Phase Fluid; 3 Nodes	Water flow in pipe
4.4	For Moist Air; 2 Nodes	Air flow across volume-control damper
4.5	For 1-Phase Fluid; 2 Nodes	Water flow across strainer
5	**Flow Divider and Inducer**	
5.1	Flow Diverger (For All Fluid)	Air at branch takeoff of main duct
5.2	Flow Multiplier (For All Fluid)	Water at inlet header to cooling coil tubings
5.3	Flow Inducer (For All Fluid)	Air across fan impeller
6	**Flow Converger**	
6.1	For Moist Air	Airstreams to AHU mixing box
6.2	For 2-Phase Fluid	Refrigerant at DX coil outlet header
6.3	For 1-Phase Fluid	Water at parallel-pumps outlet header
6.4	For Leak-in Moist Air from Outside	Duct air leakage at fan suction
7	**Flow Upon Water Spray**	
7.1	For Moist Air	Air flow in cooling tower
8	**Fluid Injection**	
8.1	Water/Steam to Moist Air	Air across humidifier injection probe
9	**Fluid Accumulator**	
9.1	For Moist Air	Air in room space
9.2	For Liquid	Water in expansion tank
10	**Heat Injection**	
10.1	To Solid	Electricity supply to heating cable
10.2	To Vapor-Generating Fluid	Vapor from heated pan humidifier
10.3	To Moist Air in Solar Collector	

(i) Thermal insulation:

$$h_o A_o(\theta_e - \theta_{s1}) + \frac{k_{12}A_{12}}{l_{12}}(\theta_{s2} - \theta_{s1}) = M_{s1}C_{s1}\frac{d\theta_{s1}}{dt} \quad (7)$$

(ii) Sheet metal:

$$\frac{k_{12}A_{12}}{l_{12}}(\theta_{s1} - \theta_{s2}) + h_i A_i(\theta_{am} - \theta_{s2}) = M_{s2}C_{s2}\frac{d\theta_{s2}}{dt} \quad (8)$$

(iii) Contained air:

$$(m_{a0}Cp_{a0} + m_{v0}Cp_{v0})\theta_{a0} - (m_{a1}Cp_{a1} + m_{v1}Cp_{v1})\theta_{a1} + h_i A_i(\theta_{s2} - \theta_{am}) = M_{am}Cp_{am}\frac{d\theta_{am}}{dt} \quad (9)$$

(iv) Leaving air (with no transport delay):

$$\theta_{a1} = \theta_{am}. \quad (10)$$

Equation 7, in its finite difference form, becomes

$$-\left[\alpha(C_{12} + C_{es}) + \frac{M_{s1}C_{s1}}{\delta t}\right]\theta_{s1} + \alpha C_{12}\theta_{s2} = \left[(1-\alpha)(C^*_{12} + C^*_{es}) - \frac{M^*_{s1}\ C^*_{s1}}{\delta t}\right]\theta^*_{s1} - (1-\alpha)C^*_{12}\ \theta^*_{s2} - [\alpha C_{es} + (1-\alpha)C^*_{es}\ \theta^*_e\ ] \quad (11)$$

where

$C_{es} = h_o A_o$,

$C_{12} = k_{12}A_{12}/l_{12}$.

Similar treatment applied to Equations 8 and 9 gives

$$\alpha C_{12}\theta_{s1} - \left[\alpha(C_{12} + C_{as}) + \frac{M_{s2}C_{s2}}{\delta t}\right]\theta_{s2} + \alpha C_{as}\theta_{am} = -(1-\alpha)C^*_{12}\ \theta^*_{s1} + \left[(1-\alpha)(C^*_{12} + C^*_{as}) - \frac{M^*_{s2}\ C^*_{s2}}{\delta t}\right]\theta^*_{s2} - (1-\alpha)\ C^*_{as}\ \theta^*_{am} \quad (12)$$

and

$$\alpha C_{as}\theta_{s2} - \left(\alpha C_{as} + \frac{M_{am}Cp_{am}}{\delta t}\right)\theta_{am} - \alpha C_{a1}\theta_{a1} + \alpha C_{a0}\theta_{a0} = -(1-\alpha)C^*_{as}\ \theta^*_{s2} + \left[(1-\alpha)C^*_{as} - \frac{M^*_{am}\ Cp^*_{am}}{\delta t}\right]\theta^*_{am} + (1-\alpha)C^*_{a1}\ \theta^*_{a1} - (1-\alpha)C^*_{a0}\ \theta^*_{a0} \quad (13)$$

where

$C_{as} = h_i A_i$,

$C_{a1} = m_{a1}Cp_{a1} + m_{v1}Cp_{v1}$,

$C_{a0} = m_{a0}Cp_{a0} + m_{v0}Cp_{v0}$.

The energy conservation matrix equation for the air duct is then given by

$$\begin{bmatrix} C(1) & C(2) & 0 & 0 & 0 \\ C(3) & C(4) & C(5) & 0 & 0 \\ 0 & C(6) & C(7) & C(8) & C(11) \\ 0 & 0 & C(9) & C(10) & 0 \end{bmatrix} \cdot \begin{bmatrix} \theta_{s1} \\ \theta_{s2} \\ \theta_{am} \\ \theta_{a1} \\ \theta_{a0} \end{bmatrix} = \begin{bmatrix} C(12) \\ C(13) \\ C(14) \\ C(15) \end{bmatrix} \quad (14)$$

If the airflow velocity is low, for a given simulation time step the distance traveled by the air can be less than the length of the duct section. Then the error introduced by Equation 10 can be significant because it merely equates the leaving air temperature to the mean (well-mixed) air temperature within the duct. For such a case θ_{am} and θ_{a1} are first evaluated separately via a transport delay subprogram, DELAY, and then substituted back into Equation 14. This subprogram determines the array of temperature distribution along the flow conduit at a future time step based on the temperature distribution at the present time step. Details of the numercial technique have been reported elsewhere (Chow 1997). Accordingly, some of the Equation 14 coefficients are modified:

$C(6) = 0$,

$C(7) = 1$,

$C(8) = 0$,

$C(9) = 0$,

$C(11) = 0$,

$C(14) = \text{DELAY}(\theta_{am})$,

$C(15) = \text{DELAY}(\theta_{a1})$.

Assuming an incompressible fluid, the flow balance for the duct dry air is given by

$$m_{a1} = m_{am} = m_{a0}. \quad (15)$$

Because condensation may occur when the inside duct surface temperature falls below the dew-point temperature of the duct air, a water vapor flow balance is also required as follows:

$$m_{v1} = m_{vm} = m_{v0} - Cc \quad (16)$$

where Cc is the rate of moisture condensation. Likewise, humidification of the airstream might occur for wetted interior surface on some other occasions.

Because of the complexity of latent heat transfer calculations, the transport delay calculations are not performed when moisture transfer takes place. While this will adversely affect accuracy in the transient response for small time-step simulations, the problem can be resolved by the use of two or more consecutive duct sections, with the initial shorter section dealing with the condensation and the subsequent longer sections the transport delay.

TABLE 2
Mass Flow Matrice Coefficients of Air Duct Model

Coefficients	First Phase	Second Phase
$C(1)$	1	1
$C(2)$	0	0
$C(3)$	0	0
$C(4)$	1	1
$C(5)$	0	0
$C(6)$	0	0
$C(7)$	1	1
$C(8)$	0	0
$C(9)$	−1	−1
$C(10)$	1	1
$C(11)$	−1	−1
$C(12)$	0	0
$C(13)$	0	0
$C(14)$	0	Cc
$C(15)$	0	0

For the first- and second-phase flows, the mass conservation matrices have the same topology as that given in Equation 14. The expressions for the equation coefficients are given in Table 2.

The air duct model overall—comprising a multi-node energy and two-phase flow conservation equation-set—can be constructed from 3 PPs:

PP	Description	Nodes Involved
1.1	Thermal conduction: solid to solid	S1, S2
2.4	Surface convection: with ambient	S1
4.1	Flow over surface: for moist air (3 nodes)	S2, AM, A1, A0

The expressions for the matrix equation coefficients, in terms of the constituent primitive part coefficients, are given in Table 3. The PP indices are 2, 2, 1, and 1 for nodes S1, S2, AM, and A1 respectively.

FAN MODEL

Airflow dynamics in fan systems are mainly due to air compressibility and fan motor dynamics (Bourdouxhe and Lebrun 1996). The flow performance of a fan is usually characterized by a performance curve that relates the total pressure rise to a polynomial expression of the mass flow rate at a definite fan speed and air density. Such a pressure rise overcomes the friction and dynamic losses at all other fan-duct system components. In a fluid flow network, the flows are related nonlinearly to the pressures at the nodes and thus require the iterative processing of a set of simultaneous nonlinear equations that are subjected to a given set of boundary conditions. The conservation of mass at each internal node is equivalent to the mathematical statement that the sum of the mass flows is equal to zero at that node. The solution technique used in ESP-r is to assign an arbitrary initial pressure to each internal node and then determine the node pressure correction vector based on a simultaneous solution of a Jacobian matrix, which represents the nodal pressure corrections in terms of all branch flow partial derivatives. The pressures are then iteratively corrected and the mass balance at each internal node is reevaluated until some convergence criterion is met. The fluid flow solver, as described, can work together with the building and plant simulation engine to handle the mass flow simulation for the plant and/or building (Clarke and Hensen 1990).

Figure 5 shows a possible finite volume model for a fan with an integral motor. Nodes S4 and S5 are solid nodes representing the motor/impeller body and fan casing, respectively. Note that the impeller and motor, here treated as a single finite volume, can be disaggregated into two or more nodes if necessity. Node A1 represents the air in contact with the motor-impeller body, node A2 represents the air in contact with the casing, node A3 represents the air at the fan exit, node A0 represents the air exiting the upstream component, and the excitation θ_e represents the ambient air temperature.

TABLE 3
Development of Insulated Air Duct Model from Primitive Part Coefficients

Matrix Coefficients		PP 1.1 Thermal Conduction (Solid to Solid) S1, S2	PP 2.4 Surface Convection (with Ambient) S1, E	PP 4.1 Flow Upon Surface (for Moist Air) S2, A1, AM, A0
$C(1)$	=	A(11,1)	+ A(24,1)	
$C(2)$	=	A(11,2)		
$C(3)$	=	A(11,3)		
$C(4)$	=	A(11,4)		+ A(41,1)
$C(5)$	=			A(41,2)
$C(6)$	=			A(41,4)
$C(7)$	=			A(41,5)
$C(8)$	=			A(41,6)
$C(9)$	=			A(41,8)
$C(10)$	=			A(41,9)
$C(11)$	=			A(41,11)
$C(12)$	=	B(11,1)	+ B(24,1)	
$C(13)$	=	B(11,2)		+ B(41,1)
$C(14)$	=			B(41,2)
$C(15)$	=			B(41,3)

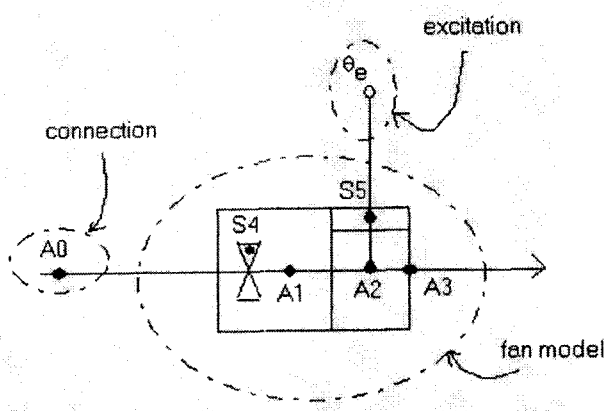

Figure 5 *Five-node model of fan with submerged motor.*

This model comprises five PPs, with one PP, No. 4.4, used twice:

PP	Description	Nodes Involved
2.4	Surface convection: with ambient	S5
4.4(1)	Flow upon surface: for moist air (2 nodes)	A0, A1, S4
4.4(2)	Flow upon surface: for moist air (2 nodes)	A1, A2, S5
5.3	Flow inducer (for all fluid)	A3
10.1	Heat injection: to solid	S4
10.3	Heat injection: to moist air	A1

The energy imparted to the airstream eventually dissipates as friction, resulting in a downstream temperature rise. This is approximated in the model by including an instantaneous energy pickup at the leaving air node given by

$$Q_\eta = \eta_W \tag{17}$$

where W is the corresponding motor power and η is the fan efficiency. Likewise, the motor inefficiency results in heat generation within the motor-impeller body:

$$Q_{1-\eta} = (1-\eta)W. \tag{18}$$

The energy conservation matrix equation for this fan model is given by

(19)

$$\begin{bmatrix} C(1) & 0 & C(2) & 0 & 0 & 0 \\ 0 & C(3) & 0 & C(4) & 0 & 0 \\ C(5) & 0 & C(6) & 0 & 0 & C(12) \\ 0 & C(7) & C(8) & C(9) & 0 & 0 \\ 0 & 0 & 0 & C(10) & C(11) & 0 \end{bmatrix} \cdot \begin{bmatrix} S4 \\ S5 \\ A1 \\ A2 \\ A3 \\ A0 \end{bmatrix} = \begin{bmatrix} C(13) \\ C(14) \\ C(15) \\ C(16) \\ C(17) \end{bmatrix}$$

where, in the case of energy balance,

$$\begin{aligned}
C(1) &= -\alpha h_{14} A_{14} - M_{s4} \cdot C_{s4} / \delta t \\
C(2) &= -\alpha h_{14} A_{14} \\
C(3) &= -\alpha (h_{e5} A_{e5} + h_{25} A_{25}) - M_{s5} \cdot C_{s5} / \delta t \\
C(4) &= \alpha h_{25} A_{25} \\
C(5) &= \alpha h_{14} A_{14} \\
C(6) &= -\alpha (m_{a1} Cp_{a1} + m_{v1} Cp_{v1} + h_{14} A_{14}) - M_{a1} \cdot Cp_{ma1} / \delta t \\
C(7) &= \alpha h_{14} A_{14} \\
C(8) &= -\alpha (m_{a0} Cp_{a0} + m_{v0} Cp_{v0}) \\
C(9) &= -\alpha (m_{a2} Cp_{a2} + m_{v2} Cp_{v2} + h_{25} A_{25}) - M_{a2} \cdot Cp_{ma2} / \delta t \\
C(10) &= -1 \\
C(11) &= 1 \\
C(12) &= \alpha (m_{a0} Cp_{a0} + m_{v0} Cp_{v0}) \\
C(13) &= [(1-\alpha) h_{14}{}^* A_{14} - M_{s4}{}^* C_{s4}{}^* / \delta t]\, \theta_{s4}{}^* - \\
&\quad (1-\alpha) h_{14}{}^* A_{14}\, \theta_{a1}{}^* + [\alpha H_{fg4}\, Cc_4 + \\
&\quad (1-\alpha) H_{fg4}{}^*\, Cc_4{}^*] - [\alpha Q_{1-h} + (1-\alpha) Q_{1-\eta}{}^*] \\
C(14) &= [(1-\alpha)(h_{e5}{}^* A_{e5} + h_{25}{}^* A_{25}) - M_{s5}{}^* C_{s5}{}^* / \delta t]\, \theta_{s5}{}^* - \\
&\quad (1-\alpha) h_{25}{}^* A_{25}\, \theta_{a2}{}^* + [\alpha H_{fg5}\, Cc_5 + \\
&\quad (1-\alpha) H_{fg5}{}^*\, Cc_5{}^*] - [\alpha h_{e5}{}^* A_{e5}\, \theta_e + \\
&\quad (1-\alpha) h_{e5}{}^* A_{e5}\, \theta_e{}^*] \\
C(15) &= [(1-\alpha)(m_{a1}{}^* Cp_{a1}{}^* + m_{v1}{}^* Cp_{v1}{}^*) - M_{a1}{}^* Cp_{ma1}{}^* / \delta t] \\
&\quad \theta_{a1}{}^* - (1-\alpha) h_{14}{}^* A_{14}\, \theta_{s4}{}^* - (1-\alpha)(m_{a0}{}^* Cp_{a0}{}^* + \\
&\quad m_{v0}{}^* Cp_{v0}{}^*)\, \theta_{a0}{}^* \\
C(16) &= [(1-\alpha)(m_{a2}{}^* Cp_{a2}{}^* + m_{v2}{}^* Cp_{v2}{}^*) - M_{a2}{}^* Cp_{ma2}{}^* / \delta t] \\
&\quad \theta_{a2}{}^* - (1-\alpha) h_{25}{}^* A_{25}\, \theta_{s5}{}^* - (1-\alpha)(m_{a1}{}^* Cp_{a1}{}^* + \\
&\quad m_{v1}{}^* Cp_{v1}{}^*)\, \theta_{a1}{}^* \\
C(17) &= 0
\end{aligned}$$

By a "mix-and-match" procedure, the expressions for the individual coefficients of this matrix equation are obtained in terms of the constituent PPs. These are given in Table 4. The PP indices are 2, 1, 1, 2, and 2 for nodes A1, A2, A3, S4, and S5, respectively.

Note that in this model the air mass flow rate can be either given as an input or treated as a variable. In the latter case, the flow is solved by ESP-r's flow network solver based on the pressure-resistance relationship at each time-step. Note also that in the PP approach, the air nodes A1, A2, and A3 cannot be combined to form one single node even though this is possible within the discretization scheme. If they were combined, then the matrix equation coefficients, when expressed in terms of the PP coefficients, would be misrepresented. Apart from this, the matrix equation template of a plant model constructed from PPs is identical to one built from a conventional finite volume conservation approach.

SIMULATION EXAMPLES

The following examples are included to illustrate the PP approach in use and to demonstrate that it is comparable to, if not better than, the conventional component-based modeling approach. It is reckoned that the conventional plant components in ESP-r have been tested via various means, including comparisons with measured data from IEA Annex (Tang 1985). The PP approach can be seen as a reimplementation of these previously validated finite volume component models.

TABLE 4
Development of Fan Model from Primitive Part Coefficients

Coefficients	PP2.4 S5	PP4.4(1) S4 A1, A0	PP4.4(2) S5, A2, A1	PP5.3 A3, A2	PP10.1 S4	PP10.3 A1
$C(1)$ =		A(44,1)			+ A(101,1)	
$C(2)$ =		A(44,2)				
$C(3)$ =	A(24,1)		+ A(44,1)			
$C(4)$ =			A(44,2)			
$C(5)$ =		A(44,3)				
$C(6)$ =		A(44,4)				
$C(7)$ =			A(44,3)			
$C(8)$ =			A(44,6)			
$C(9)$ =			A(44,4)			
$C(10)$ =				A(53,2)		
$C(11)$ =				A(53,1)		
$C(12)$ =		A(44,6)				
$C(13)$ =		B(44,1)			+ B(101,1)	
$C(14)$ =	B(24,1)		+ B(44,1)			
$C(15)$ =		B(44,2)				+ B(103,1)
$C(16)$ =			+ B(44,2)			
$C(17)$ =				B(53,1)		

A match of simulation results serves to verify the validity of the PP approach used in the construction of finite volume component models.

Fan-Duct System

Figure 6 details a fan-duct system serving an industrial plant. The system draws in outside air to the plant room at a constant volume flow rate. The required operating states were chosen according to practical design standards. The industrial plant operates on a 24-hour basis and gives rise to a sinusoidal heat load that varies between 10 and 20 kW within a period of 4 hours. The objective of the simulation is to determine the daily variation in plant room temperature under warm ambient conditions.

Two separate simulation runs were performed, one utilizing conventional finite volume component models for the fan and duct components (ESP-r models 30 and 60, respectively) and the other utilizing component models built from PPs (models 560 and 580, respectively). The time step for both simulations was two minutes, which yielded consistently stable solutions. Figure 7 shows the predicted daily variation

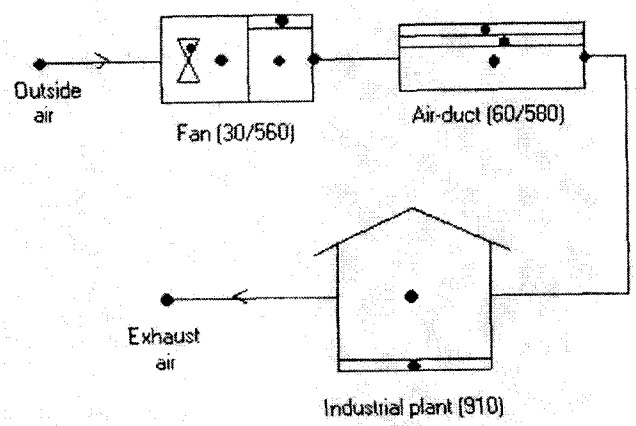

Figure 6 Supply ventilation system network.

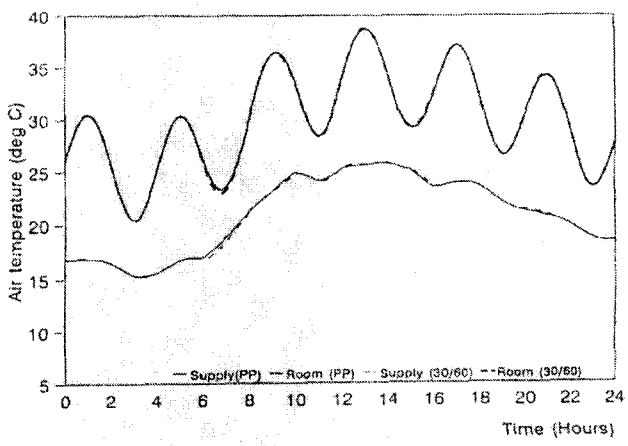

Figure 7 Comparison of daily temperature variations.

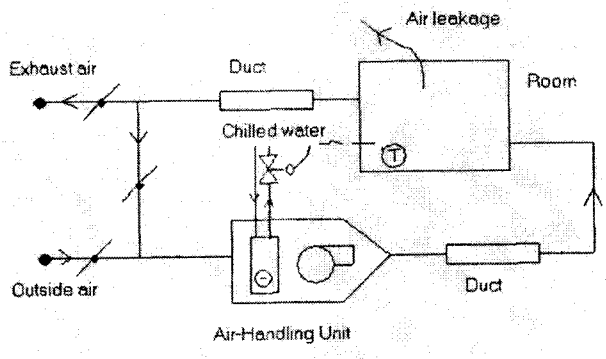

Figure 8 A cooling-only CAV system.

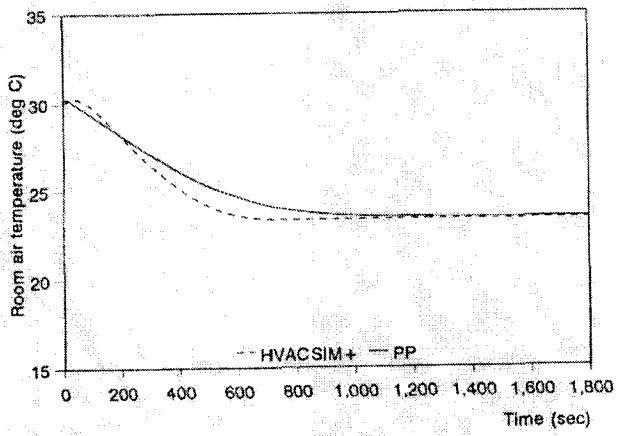

Figure 9 Comparison of dynamic response of room temperature during plant start-up.

of supply and plant room temperatures. As can be seen, the results are almost identical.

Air-Conditioning System

Figure 8 shows the configuration of a cooling-only CAV system, with a remote AHU plant delivering supply air at a constant flow rate of 2.5 kg/s, resulting in a positive pressure inside the air-conditioned space. The return and outdoor airstreams mix at a fixed ratio. Chilled-water flow is proportionally controlled by a room thermostat set at 24°C. The objective of the simulation is to predict, for a warm condition, the transient response of room air temperature during plant start-up at 30°C and under a steady thermal load.

Two separate simulation runs were performed, one using HVACSIM+, a component modular simulation program (Clark 1985), and the other, the ESP-r program with the plant components built from the PP models. In the latter case, the cooling coil was represented by a 16-node explicit model comprising four interconnected air-to-water heat-transfer tubes in counterflow arrangement (Chow 1995b). Each heat-transfer tube is a four-node model. A time-step of one second was used. Figure 9 compares the simulation results. As can be seen, the predictions are in line.

CONCLUSIONS

Primitive part (PP) modeling provides a means to improve and control the integrity of component models. Plant component models developed from PPs are fundamental by nature, with explicit physical meaning and a clear mathematical structure. This paper has explained the theoretical basis of the PP approach in terms of fan and air duct models. The mathematical models that result have been shown to be equivalent to the corresponding models developed on the basis of formal conservation principles applied to finite volumes and to produce agreement with results from the HVACSIM+ program. The principal benefit of the approach lies in its flexibility and the prospect it affords for the synthesis of component models based on physical component descriptions.

REFERENCES

Aasem, E.O. 1993. Practical simulation of building and air-conditioning systems in the transient domain. Ph.D. thesis, Energy Systems Research Unit, Department of Mechanical Engineering, University of Strathclyde, Scotland.

Bourdouxhe, J., and J. Lebrun. 1996. Reference guide for dynamic models of HVAC. Prepared for TC 4.6 Project Monitoring Subcommittee, ASHRAE Research Project 738-TRP, American Society of Heating, Refrigerating and Air-Conditioning Engineers, Inc.

Bring, A., P. Sahlin, and E.F. Sowell. 1992. The neutral model format for building simulation. Department of Building Services Engineering, Royal Institute of Technology, Stockholm, Sweden.

Buhl, W.F., A.E. Erdem, F.C. Winkelmann, and E. F. Sowell. 1993. Recent improvements in SPARK: Strong component decomposition, multivalued objects, and graphical interface. *Proc. Building Simulation '93, University of Adelaide, Australia*, pp. 283-9.

Chow, T.T. 1993. A plant component taxonomy for ESP-r simulation environment. *Proc. Building Simulation '93, University of Adelaide, Australia*, pp. 429-34.

Chow, T.T. 1995. Generalization in plant component modelling. *Proc. Building Simulation '95, University of Wisconsin, Madison, USA*, pp. 48-55.

Chow, T.T. 1995a. Air-conditioning plant component taxonomy by primitive parts. Ph.D. thesis, Energy Systems Research Unit, Department of Mechanical Engineering, University of Strathclyde, Scotland.

Chow, T.T. 1997. Chilled water cooling coil models from empirical to fundamental. *Numerical Heat Transfer, Part A: Applications*, Vol. 32, pp. 63-83.

Chow, T.T., J.A. Clarke, and A. Dunn. 1997. Primitive parts: An approach to air-conditioning component modelling. *Energy and Buildings* 26: 165-173.

Clark, D.R. 1985. HVACSIM+, Building systems and equipments simulation program reference manual. U.S. Department of Commerce, NBSIR-2996.

Clarke, J.A. 1977. Environmental systems performance. Ph.D. thesis, Department of Architecture and Building Science, University of Strathclyde, Scotland.

Clarke, J.A. 1985. *Energy simulation in building design.* Bristol and Boston: Adam Hilger Ltd.

Clarke, J.A. 1986. The energy kernel system. *Proc. 2d Int. Conf. on System Simulation in Buildings, University of Liege, Belgium*, pp. 455-470.

Clarke, J.A., and J.L.M. Hensen. 1990. A fluid flow network solver for integrated building and plant energy simulation. *Proc. 3rd Int. Conf. on System Simulation in Buildings, University of Liege, Belgium*, pp. 151-167.

Clarke, J.A., and D. MacRandal. 1993. The energy kernel system: Form and Content. *Proc. Building Simulation '93, University of Adelaide, Australia*, pp. 307-315.

ESRU. 1995. ESP-r: A building energy simulation environment, User guide version 9 Series. Energy Systems Research Unit, Department of Mechanical Engineering, University of Strathclyde, Scotland.

McLean, D.J. 1982. The simulation of solar energy systems. Ph.D. thesis, Department of Architecture and Building Science, University of Strathclyde, Scotland.

Mitchell, J. 1997. Simulation or experimentation for HVAC systems? Foreword of *International Journal of Heating, Ventilating, Air-Conditioning and Refrigeration Research* 3 (1): 1.

Ogata, K. 1992. *System dynamics*, 2d ed. Prentice-Hall, Inc.

Sahlin, P., A. Bring, and K. Kolsaker. 1995. Future trends of the neutral model format (NMF). *Proc. Building Simulation '95, University of Wisconsin, Madison, USA*, pp. 737-544.

Sowell, E.F. 1991. Next generation building services engineering software opportunities for the practitioner. *Proc. Building Environmental Performance '91, Canterbury, UK*, pp. 1-9.

Sowell, E.F., and M.A. Moshier. 1995. HVAC component model libraries for equation-based solvers. *Proc. Building Simulation '95, University of Wisconsin, Madison, USA*, pp. 189-196.

Tang, D. 1985. The simulation of wet central heating systems. Ph.D. thesis, Department of Architecture and Building Science, University of Strathclyde, Scotland.

NOMENCLATURE

A	= area
C	= specific heat capacity
Cc	= moisture condensation rate
Cp	= specific heat at constant pressure
g	= moisture content
H	= specific enthalpy
h	= heat transfer coefficient
k	= thermal conductivity
Kd	= mass diffusion coefficient
l	= length; spacing
M	= mass
m	= mass flow rate
Ni	= primitive part connection index
Q	= heat flux
S	= solid
t	= time
U	= overall heat transfer coefficient
W	= power
x	= dryness fraction
α	= weighting factor
η	= efficiency
θ	= temperature

SUPERSCRIPT

*	= present time row

SUBSCRIPTS

a	= air (dry)
dew	= dew point
e	= ambient
fg	= latent exchange
i	= internal
m	= mean
ma	= moist air
o	= external
s	= solid
sat	= saturated
v	= water vapour
w	= liquid water or wet

APPENDIX

Part No. 1.1 Thermal Conduction (Solid to Solid)

2 No. of Nodes:
M - solid
N - solid

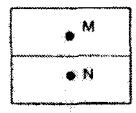

Energy flow matrix:

$$\begin{bmatrix} A(11,1) & A(11,2) \\ A(11,3) & A(11,4) \end{bmatrix} \cdot \begin{bmatrix} \theta_m \\ \theta_n \end{bmatrix} = \begin{bmatrix} B(11,1) \\ B(11,2) \end{bmatrix}$$

where

$$A(11,1) = -\alpha C_{mn} - M_m C_m/(Ni_m \delta t)$$

$$A(11,2) = a C_{mn}$$

$$A(11,3) = \alpha C_{mn}$$

$$A(11,4) = -\alpha C_{mn} - M_n C_n/(Ni_n \delta t)$$

$$B(11,1) = [(1-\alpha) C_{mn}^* - M_m^* C_m^*/(Ni_m \delta t)]\theta_m^* - (1-\alpha) C_{mn}^* \theta_n^*$$

$$B(11,2) = [(1-\alpha) C_{mn}^* - M_n^* C_n^*/(Ni_n \delta t)]\theta_n^* - (1-\alpha) C_{mn}^* \theta_m^*.$$

Mass flow matrices (for both first- and second-phase mass balances):

$A(11,1) = 1/Ni_m$

$A(11,2) = 0$

$A(11,3) = 0$

$A(11,4) = 1/Ni_n$

$B(11,1) = 0$

$B(11,2) = 0.$

Part No. 2.1 Surface Convection (with Moist Air)

2 Nos. of Nodes:
S - solid
A - moist air

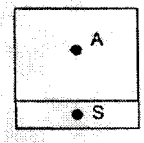

Energy flow matrix:

$$\begin{bmatrix} A(21,1) & A(21,2) \\ A(21,3) & A(21,4) \end{bmatrix} \begin{bmatrix} \theta_s \\ \theta_a \end{bmatrix} = \begin{bmatrix} B(21,1) \\ B(21,2) \end{bmatrix}$$

where

$A(21,1) = -\alpha C_{as} - M_s \cdot C_s/(Ni_s \cdot \delta t)$

$A(21,2) = \alpha C_{as}$

$A(21,3) = \alpha C_{as}$

$A(21,4) = -\alpha C_{as} - M_\alpha \cdot Cp_{ma}/(Ni_a \cdot \delta t)$

$B(21,1) = [(1-\alpha) C_{as}^* - M_s^* C_s^*/(Ni_s\, \delta t)]\theta_s^* - (1-\alpha) C_{as}^* \theta_a^* + [\alpha C_{fg} + (1-\alpha) C_{fg}^*]$

$B(21,2) = [(1-\alpha) C_{as}^* - M_a^* Cp_{ma}^*/(Ni_a\, \delta t)]\theta_a^* - (1-\alpha) C_{as} \theta_s^*$

and

$C_{fg} = -H_{fg}\, Cc.$

Mass flow matrices:

	First-phase (dry air)	Second-phase (water vapor)
$A(21,1)$	$1/Ni_s$	$1/Ni_s$
$A(21,2)$	0	0
$A(21,3)$	0	0
$A(21,4)$	$1/Ni_a$	$1/Ni_a$
$B(21,1)$	0	0
$B(21,2)$	0	$-Cc$

and

$Cc = 0$ for dry surface, i.e., when $\theta_s > \theta_a dew$ and $M_w = 0$;

$= Kd\, A_{as}\, (g_a - g_s)$ for wet surface, i.e., $M_w > 0$

where M_w is the amount of condensate on the surface, g_s is the saturated moist content at θ_s.

Part No. 2.4 Surface Convection (with Ambient)

1 No. of Node:
S - solid (or fluid)

1 No. of Boundary Condition:
E - boundary fluid

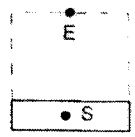

Energy flow matrix:

$$[A(24,1)] \cdot [\theta_s] = [B(24,1)]$$

where

$A(24,1) = -\alpha C_{es} - M_s \cdot C_s/(Ni_s \cdot \delta t)$

$B(24,1) = [(1-\alpha) C_{es}^* - M_s^* C_s^*/(Ni_s\, \delta t)]\theta_s^* - [\alpha C_{es}\, \theta_e + (1-\alpha) C_{es}^* \theta_e^*].$

Mass flow matrices (for both first- and second-phase):

$A(24,1) = 1/Ni_s$

$B(24,1) = 0.$

Notes:

1. The thermal state of the boundary fluid in bulk is taken as not controllable by the heat exchange with the surface; θ_e thus becomes an external excitation and its value during the simulation period is user specified.
2. The possibility of mass exchange (e.g., condensation) on the surface is not considered.

Part No. 3.1 Surface Radiation (with Local Surface)

2 Nos. of Nodes:
S - solid surface
T - solid surface

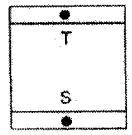

Energy flow matrix:

$$\begin{bmatrix} A(31,1) & A(31,2) \\ A(31,3) & A(31,4) \end{bmatrix} \cdot \begin{bmatrix} \theta_s \\ \theta_t \end{bmatrix} = \begin{bmatrix} B(31,1) \\ B(31,2) \end{bmatrix}$$

where

$A(31,1) = -\alpha C_{st} - M_s \cdot C_s/(Ni_s \cdot \delta t)$

$A(31,2) = \alpha C_{st}$

$A(31,3) = \alpha C_{st}$

$A(31,4) = -\alpha C_{st} - M_t \cdot C_t/(Ni_t \cdot \delta t)$

$B(31,1) = [(1-\alpha) C_{st}^* - M_s^* C_s^*/(Ni_s\, \delta t)]\theta_s^* - (1-\alpha) C_{st}^* \theta_t^*$

$B(31,2) = [(1-\alpha) C_{st}^* - M_t^* C_t^*/(Ni_t\, \delta t)]\theta_t^* - (1-\alpha) C_{st}^* \theta_s^*.$

Mass flow matrices (for both first- and second-phase):

$A(31,1) = 1/Ni_s$

$A(31,2) = 0$

$A(31,3) = 0$

$A(31,4) = 1/Ni_t$

$B(31,1) = 0$

$B(31,2) = 0.$

Part No. 4.1 Flow Upon Surface (for Moist Air; 3 Nodes)

3 Nos. of Nodes:
S - solid surface
AM - moist air in contact
A1 - leaving moist air
1 No. of Connection:
A0 - incoming moist air

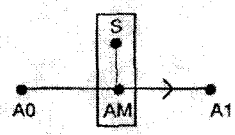

Energy flow matrix:

$$\begin{bmatrix} A(41,1) & A(41,2) & 0 & 0 \\ A(41,4) & A(41,5) & A(41,6) & A(41,11) \\ 0 & A(41,8) & A(41,9) & 0 \end{bmatrix} \cdot \begin{bmatrix} \theta_s \\ \theta_{am} \\ \theta_{a1} \\ \theta_{a0} \end{bmatrix} = \begin{bmatrix} B(41,1) \\ B(41,2) \\ B(41,3) \end{bmatrix}$$

where

$A(41,1) = -\alpha C_{as} - (M_s C_s / Ni_s \cdot \delta t)$
$A(41,2) = \alpha C_{as}$
$A(41,4) = \alpha C_{as}$
$A(41,5) = -\alpha C_{as} - M_a Cp_{ma} / Ni_{a1} \cdot \delta t$
$A(41,6) = -\alpha C_{a1}$
$A(41,8) = -1$
$A(41,9) = 1$
$A(41,11) = \alpha C_{a0}$
$A(41,12) = 0$
$B(41,1) = [(1-\alpha) C_{as}{}^* - M_s{}^* C_s{}^* / (Ni_s \delta t)]\theta_s{}^* - (1-\alpha) C_{as}{}^* \theta_{a1}{}^* + [\alpha C_{fg} + (1-\alpha) C_{fg}{}^*]$
$B(41,2) = [(1-\alpha) C_{as}{}^* - M_a{}^* Cp_{ma}{}^* / (Ni_{a1} \delta t)]\theta_{am}{}^* - (1-\alpha) C_{as}{}^* \theta_s{}^* - (1-\alpha) C_{a0}{}^* \theta_{a0}{}^* - (1-\alpha) C_{a1}{}^* \theta_{a1}{}^*$
$B(41,3) = 0$

and

$C_{fg} = -H_{fg} (m_{v0} - m_{v1}) = -H_{fg} Cc.$

For dry surface, $m_{v1} = m_{v0}$, so $C_{fg} = 0$.

In case the DELAY flag is ON, the following coefficients will be revised as

$A(41,4) = 0$
$A(41,5) = 1$
$A(41,6) = 0$
$A(41,4) = 0$
$A(41,8) = 0$
$A(41,11) = 0$
$B(41,2) = \text{DELAY}(\theta_{am})$
$B(41,3) = \text{DELAY}(\theta_{a1})$.

Mass flow matrices:

	First-phase (dry air)	Second-phase (water vapor)
$A(41,1)$	$= 1/Ni_s$	$1/Ni_s$
$A(41,2)$	$= 0$	0
$A(41,4)$	$= 0$	0
$A(41,5)$	$= 1/Ni_{am}$	$1/Ni_{am}$
$A(41,6)$	$= 0$	0
$A(41,8)$	$= -1$	-1
$A(41,9)$	$= 1$	1
$A(41,11)$	$= -1$	-1
$B(41,1)$	$= 0$	0
$B(41,2)$	$= 0$	$-Cc$
$B(41,3)$	$= 0$	0

where

$Cc = 0$ for dry surface, i.e., when $\theta_s > \theta_{a0}$dew and $M_w = 0$;
$= Kd A_{as} (g_{am} - g_s)$ for wet surface, i.e., $M_w > 0$

where M_w is the amount of condensate on the surface, g_s is the saturated moist content at θ_s.

Part No. 4.4 Flow Upon Surface (for Moist Air; 2 Nodes)

2 Nos. of Nodes:
S - solid surface
A1 - leaving moist air
1 No. of Connection:
A0 - incoming moist air

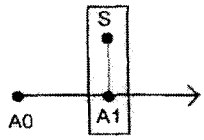

Energy flow matrix:

$$\begin{bmatrix} A(44,1) & A(44,2) & 0 \\ A(44,3) & A(44,4) & A(44,6) \end{bmatrix} \cdot \begin{bmatrix} \theta_s \\ \theta_{a1} \\ \theta_{a0} \end{bmatrix} = \begin{bmatrix} B(44,1) \\ B(44,2) \end{bmatrix}$$

where

$A(44,1) = -\alpha C_{as} - M_s C_s / (Ni_s \cdot \delta t)$
$A(44,2) = \alpha C_{as}$
$A(44,3) = \alpha C_{as}$
$A(44,4) = -\alpha (C_{a1} + C_{as}) - (M_a Cp_{ma} / Ni_{a1} \cdot \delta t)$
$A(44,6) = \alpha C_{a0}$
$B(44,1) = [(1-\alpha) C_{as}{}^* - M_s{}^* C_s{}^* / (Ni_s \delta t)]\theta_s{}^* - (1-\alpha) C_{as}{}^* \theta_{a1}{}^* + [\alpha C_{fg} + (1-\alpha) C_{fg}{}^*]$
$B(44,2) = [(1-\alpha)(C_{a1}{}^* + C_{as}{}^*) - M_a{}^* Cp_{ma}{}^* / (Ni_{a1} \delta t)]\theta_{a1}{}^* - (1-\alpha) C_{as}{}^* \theta_s{}^* - (1-\alpha) C_{a0}{}^* \theta_{a0}{}^*$

and

$C_{fg} = -H_{fg} (m_{v0} - m_{v1}) = -H_{fg} Cc.$

For dry surface, $m_{v1} = m_{v0}$, so $C_{fg} = 0$.

Mass flow matrices:

	First-phase (dry air)	Second-phase (water vapor)
$A(44,1)$	$= 1/Ni_s$	$1/Ni_s$
$A(44,2)$	$= 0$	0
$A(44,3)$	$= 0$	0
$A(44,4)$	$= 1/Ni_{a1}$	$1/Ni_{a1}$

$A(44,6) = -1$ $\quad -1$

$B(44,1) = 0$ $\quad 0$

$B(44,2) = 0$ $\quad -Cc$

where

$Cc = 0$ for dry surface, i.e., when $\theta_s > \theta_{a0}$ dew and $M_w = 0$;

$= Kd\, A_{as}\, (g_{a1} - g_s)$ for wet surface, i.e., $M_w > 0$

where M_w is the amount of condensate on the surface, g_s is the saturated moist content at θ_s.

Part No. 5.3 Flow Inducer (for All Fluid Types)

1 Nos. of Nodes:

R1 - leaving fluid

1 No. of Connection:

R0 - incoming fluid

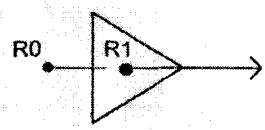

Energy flow matrix:

$$[A(53,1)\ \ A(53,2)] \cdot \begin{bmatrix} \theta_{r1} \\ \theta_{r0} \end{bmatrix} = [B(53,1)]$$

where

$A(53,1) = 1$

$A(53,2) = -1$

$B(53,1) = 0.$

Mass flow matrices:

	First phase	Second phase
$A(53,1)$	$= 1$	1
$A(53,2)$	$= 0$	0
$B(53,1)$	$= k_1\, m_i$	$k_2\, m_i$

Note:

1. m_i is the induced mass flow rate.
2. The values of k_1 and k_2 are fluid-type dependent such that:

Fluid-type	Moist Air	Liquid	Wet Vapor	Dry Vapor
k_1	1	1	1−x	0
k_2	g_{a0}	0	x	1

where $g_{a0} = m_{v0}/m_{a0}$ and $x = m_{v0}/(m_{w0} + m_{v0})$.

Part No. 10.1 Heat Injection (to Solid)

1 No. of Node:

S - solid

1 No. of Excitation:

Q - heat input

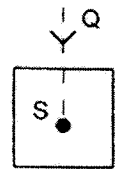

Energy flow matrix:

$$[A(101,1)] \cdot [\theta_s] = [B(101,1)]$$

where

$A(101,1) = -M_s \cdot C_s/(Ni_s \cdot \delta t)$

$B(101,1) = -[M_s{}^*C_s{}^*/(Ni_s \cdot \delta t)]\, \theta_s{}^* - [\alpha Q + (1-\alpha)Q^*].$

Mass flow matrices (for both first- and second-phase):

$A(101,1) = 1/Ni_s$

$B(101,1) = 0.$

Part No. 10.3 Heat Injection (to Moist Air)

1 No. of Node:

A - moist air

1 No. of Excitation:

Q - heat input

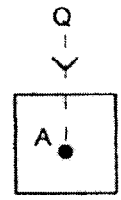

Energy flow matrix:

$$[A(103,1)] \cdot [\theta_a] = [B(103,1)]$$

where

$A(103,1) = -[\alpha C_a + (1-\alpha)C_a{}^*]/(Ni_a \cdot \delta t)$

$B(103,1) = -[\alpha C_a + (1-\alpha)C_a{}^*]\, \theta_a{}^*/(Ni_a \cdot \delta t) - [\alpha Q + (1-\alpha)Q^*] - [\alpha H_{fg}\, Cc + (1-\alpha)H_{fg}{}^*\, Cc^*]$

and

Cc = condensation rate $= (M_v{}^* - M_v)/\delta t;$

$C_a = M_a\, Cp_a + M_v\, Cp_v$

Note: Check $g_a = M_v / M_a$ against $g_a sat$ at each time step; if $g_a > g_a sat$, then $M_v = M_a \cdot g_a sat$.

Mass flow matrices (for both first- and second-phase):

$A(103,1) = 1/Ni_a$

$B(103,1) = 0.$